J. Fluid Mech. (1999), *vol.* 391, *pp.* 1–27. Printed in the United Kingdom

The unsteady expansion and contraction of a long two-dimensional vapour bubble between superheated or subcooled parallel plates

By S. K. WILSON[1], S. H. DAVIS[2] AND S. G. BANKOFF[3]

[1] Department of Mathematics, University of Strathclyde, Livingstone Tower, 26 Richmond Street, Glasgow G1 1XH, UK

[2] Department of Engineering Sciences and Applied Mathematics, Robert R. McCormick School of Engineering and Applied Science, Northwestern University, 2145 Sheridan Road, Evanston, IL 60208, USA

[3] Department of Chemical Engineering, Robert R. McCormick School of Engineering and Applied Science, Northwestern University, 2145 Sheridan Road, Evanston, IL 60208, USA

(Received 5 June 1998 and in revised form 16 November 1998)

In an attempt to model the growth and collapse of a vapour bubble in nucleate boiling this paper investigates the unsteady expansion and contraction of a long two-dimensional vapour bubble confined between superheated or subcooled parallel plates whose motion is driven by mass-transfer effects due to evaporation from the liquid to the vapour and condensation from the vapour to the liquid. It is shown that in the asymptotic limit of strong surface tension (small capillary number) the solution consists of two capillary-statics regions (in which the bubble interface is semicircular at leading order) and two thin films attached to the plates, connected by appropriate transition regions. This generalization of the steady and isothermal problem addressed by Bretherton (1961) has a number of interesting physical and mathematical features. Unlike in Bretherton's problem, the bubble does not translate but can change in size. Furthermore, the thin films are neither spatially nor temporally uniform and may dry out locally, possibly breaking up into disconnected patches of liquid. Furthermore, there is a complicated nonlinear coupling with a delay character between the profiles of the thin films and the overall expansion or contraction of the bubble which means that the velocity with which the bubble expands or contracts is typically not monotonic. This coupling is investigated for three different combinations of thermal boundary conditions and two simple initial thin-film profiles. It is found that when both plates are superheated equally the bubble always expands, and depending on the details of the initial thin-film profiles, this expansion may either continue indefinitely or stop in a finite time. When both plates are subcooled equally the bubble always contracts, and the length of the thin-film region always approaches zero asymptotically. When one plate is superheated and the other subcooled with equal magnitude the bubble may either expand or contract initially, but eventually the bubble always contracts just as in the pure-condensation case.

1. Introduction

In his pioneering paper Bretherton (1961) investigated the steady translation of a long axisymmetric and isothermal bubble of inviscid gas surrounded by a viscous liquid and confined within a cylindrical tube. Bretherton analysed the problem in

the asymptotic limit of strong surface tension (small capillary number) and showed that the leading-order solution is composed of two 'capillary-statics' regions at the ends of the bubble (in which the bubble interface is semi-spherical) which merge through 'transition' regions into a quiescent thin film of uniform thickness attached to the tube in the middle of the bubble. Bretherton's analysis also applies to semi-infinite bubbles and can be readily adapted to describe two-dimensional bubbles confined between parallel plates. Although Bretherton himself was apparently unaware of their work, his solution has many similarities to that obtained earlier by Landau & Levich (1942) to describe the thin film adhering to a flat plate withdrawn from a bath of viscous liquid (the drag-out or dip-coating problem). Bretherton's approach has been formalized and extended by Park & Homsy (1984) and subsequent authors. As Bretherton himself was aware, his theoretical expression for the thickness of the thin film underpredicts the experimental results at small capillary number, precisely where the theory should be most accurate. Bretherton (1961) and Schwartz, Princen & Kiss (1986) discussed several possible causes for this disagreement, but the first complete explanation was provided by Ratulowski & Chang (1990) who demonstrated that the presence of surface-tension gradients caused by small amounts of surface contaminant were capable of accounting for the discrepancy. The experiments reported by Schwartz *et al.* (1986) also showed that the thickness of the thin film is strongly dependent on the length of the bubble (a feature absent from Bretherton's solution, which is independent of the bubble's length) and subsequently Park (1992) demonstrated that this could also be explained by the presence of surface contaminant. Surface-tension gradients arising from surface contaminant are not a concern for a pure vapour in contact with its pure condensate, as shall be considered in the present work. However, they may be of considerable importance in considering the multicomponent mixtures which often occur in practice.

The insights gained from studying the solution of Bretherton's problem are important in many different physical contexts, including several coating processes, flow in porous media and even biological systems, and as a result Bretherton's work has received considerable attention since its publication. For example, subsequent workers have sought to incorporate additional physical effects into the basic problem, notably Wilson (1995) who investigated the effect of a constant axial temperature gradient on the steady motion of a droplet in a heated tube.

In Bretherton's problem the mass of the bubble is constant and the steady translation is driven by an externally imposed pressure gradient. The present paper investigates the alternative problem of the unsteady expansion and contraction of a long two-dimensional vapour bubble confined between superheated or subcooled parallel plates whose motion is driven by mass-transfer effects due to evaporation from the liquid to the vapour and condensation from the vapour to the liquid. This system has a number of interesting physical and mathematical features. Since the motion will be, in general, unsteady, the thin films will not be deposited with constant thicknesses. Furthermore, the superheating or subcooling of the plates will cause the profiles of the thin films to evolve after they have been deposited and may cause a film on a superheated plate to dry out locally at various places and times, possibly breaking up into disconnected patches of liquid as it dries. Since the mass transfer depends on the shape of the bubble interface, which itself depends on the past history of the motion, there is a complicated nonlinear coupling with a delay character between the profiles of the thin films and the overall expansion and contraction of the bubble. The present work identifies this coupling and investigates its consequences.

Our main motivation for studying this problem is to develop a simple model which captures some of the main features of the growth and collapse of a vapour bubble attached to a superheated wall in nucleate boiling. It has long been recognized that typically a thin film of liquid (the microlayer) is left behind on the wall as such a vapour bubble grows. The subsequent rapid evaporation of the microlayer may supply the bulk of the vapour to the growing bubble and hence determine the dynamics of the bubble growth and collapse as well as the local heat transfer. Experimental measurement of the microlayer have been reported by Jawurek (1969), Cooper & Lloyd (1969), Voutsinos & Judd (1975) and Koffman & Plesset (1983). Several authors, notably Cooper (1969), Cooper & Lloyd (1969), Snyder & Robin (1969), Robin & Snyder (1970), Kotake (1970), Van Ouwerkerk (1971), Guy & Ledwidge (1973), Van Stralen *et al.* (1975), Plesset & Prosperetti (1976), Zijl, Ramakers & Van Stralen (1979), Lee & Nydahl (1989), Tsung-Chang & Bankoff (1990), Guo & El-Genk (1994) and Mei, Chen & Klausner (1995*a*,*b*) have developed approximate and numerical models of varying sophistication for a vapour bubble incorporating a microlayer. However, despite considerable theoretical and experimental effort, the understanding of the process remains incomplete. In the situation considered in the present paper, as often in nucleate boiling, the mass transfer is dominated by that from and to the thin films on the superheated or subcooled walls. The present model does not address the processes of bubble nucleation, periodic bubble growth and collapse, and bubble departure from the superheated wall, all of which are beyond the scope of the present work. Dhir (1998) reviews some of the recent developments in understanding boiling phenomena.

The present problem also has application to a number of other physical situations. For example, many practical coating processes involve evaporating liquid films which eventually form solid coatings and which may dry out prematurely causing coating imperfections. Furthermore, penetration of vapour bubbles into heated capillaries is of interest in the study of heat-generating porous materials, such as radioactive debris beds in severe nuclear accident scenarios.

The behaviour of the thin liquid film on the superheated or subcooled plates is central to the present problem. Reviews of the extensive literature on thin-film flows have been given recently by Bankoff (1994), Oron, Davis & Bankoff (1997) and Myers (1998). Of particular interest here is the work on evaporating and condensing films. Burelbach, Bankoff & Davis (1988) formulated and analysed the general evolution equation for a thin evaporating or condensing liquid film on a superheated or subcooled horizontal plate including mass loss, vapour recoil, thermocapillary, surface tension, gravity and long-range intermolecular attraction effects. Panzarella, Davis & Bankoff (1997) recently formulated and analysed the corresponding evolution equation for the thin vapour film which develops between an evaporating liquid and a superheated plate in horizontal film boiling. Wilson (1993) and Howison *et al.* (1997) used a thin-film model to analyse the sometimes-unexpected behaviour of a drying paint layer consisting of evaporating and non-evaporating components and found excellent agreement with earlier experimental observations. The local dry-out of an evaporating liquid film typically involves moving contact lines. Several workers, including Potash & Wayner (1972), Renk & Wayner (1979*a*,*b*), Moosman & Homsy (1980), Wayner & Schonberg (1992), Wayner (1993) and DasGupta *et al.* (1993) have examined the details of the flow in the vicinity of a contact line with evaporation and condensation. Taking a somewhat different approach, Anderson & Davis (1995) formulated a macroscopic contact-line condition representing a leading-order superposition of spreading and evaporative effects which generalizes the model

used by Ehrhard & Davis (1991) for non-evaporative spreading and used it to study the spreading of an evaporating droplet on a heated plate.

The structure of the present paper is as follows. In § 2 the model is formulated. In § 3 the special case of a continuous thin film is considered and the problem in this case formulated as an integro-delay equation with non-constant delay. In § 4 this delay-equation formulation is used to analyse the stability of a simple solution corresponding to a bubble expanding at constant velocity. In § 5 the numerical method used to solve the full problem is described and in §§ 6, 7 and 8 solutions to the model in the cases when both plates are superheated equally, both plates are subcooled equally and when one plate is superheated and the other subcooled with equal magnitude, respectively, are described. Finally, in § 9 the results are summarized and directions for future work are suggested.

2. Problem formulation

Consider the unsteady expansion and contraction of a long two-dimensional bubble of inviscid and incompressible vapour with density $\rho^{(V)}$ surrounded by its condensate, an incompressible Newtonian liquid with constant dynamic viscosity μ, kinematic viscosity ν, density ρ, thermal diffusivity κ and thermal conductivity k, and confined between two infinitely wide parallel horizontal solid plates a distance $2d$ apart. The constant surface tension at the interface of the bubble is denoted by σ; the effect of gravity is neglected. The upper and lower plates are held at (in general different) uniform temperatures T_u and T_l, respectively, which may be either above or below the saturation temperature T_s. This superheating or subcooling will cause evaporation from the liquid to the vapour or condensation from the vapour to the liquid and hence the bubble will expand or contract in an unsteady manner that needs to be determined.

In this paper only two-dimensional bubbles symmetric about a vertical axis are considered and Cartesian coordinates (x, y) are chosen so that the plates are at $y = \pm d$ and only the half of the bubble lying in $x \geqslant 0$ is considered. For simplicity of presentation in much of the derivation that follows, attention is confined to the lower quarter of the bubble lying in $x > 0$, $y < 0$; the corresponding results for the upper quarter of the bubble lying in $x > 0$, $y > 0$ can then be obtained immediately.

In the asymptotic limit of strong surface tension (small capillary number) it will be shown that the liquid–vapour interface in $x > 0$, $y < 0$ is composed of the three different regions shown in figure 1, namely a 'capillary-statics' region in $R(t) < x < R(t) + S(t)$, a 'transition' region near $x = R(t)$ and a 'thin-film' region in $0 < x < R(t)$ in which the liquid film may dry out locally, possibly breaking up into disconnected patches; the functions $R = R(t)$ and $S = S(t)$ will be determined as part of the solution. Three specific problems shall be addressed as in figure 1: both plates superheated (specifically, $T_u = T_l = T_s + \Delta T$), both plates subcooled ($T_u = T_l = T_s - \Delta T$), and the lower plate superheated and the upper plate subcooled with equal magnitude ($T_u = T_s - \Delta T$, $T_l = T_s + \Delta T$), where $\Delta T > 0$ is the magnitude of the superheating or subcooling.

The interfacial conditions appropriate at an evaporating or condensing interface were discussed in detail by Burelbach *et al.* (1988); here the results relevant to the present problem are summarized. Note that Burelbach *et al.* (1988) included several additional physical effects (namely vapour recoil, thermocapillary and long-range intermolecular attraction effects) which are omitted from the present description for simplicity, but could, in principle, also be included. Burelbach *et al.*'s (1988) 'one-sided'

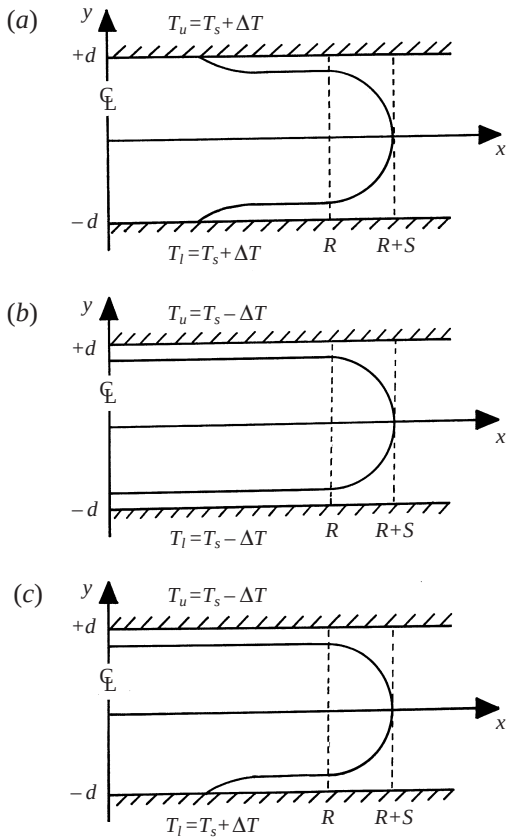

FIGURE 1. Geometry of the three problems considered: (*a*) both plates superheated, (*b*) both plates subcooled and (*c*) the lower plate superheated and the upper plate subcooled. Note that in all three cases the bubble is symmetric about the y-axis and so only the half of the bubble lying in $x \geqslant 0$ is shown.

model is adopted in which, in the same spirit as the Boussinesq approximation of thermal convection, one considers the limiting case in which the density, viscosity and thermal conductivity of the liquid are all much greater than those of the vapour, but the vapour density in the mass balance at the interface is retained where it multiplies the (large) vapour velocity.

In order to describe this situation length, velocity, time, pressure and temperature difference from T_s are non-dimensionalized with d, v/d, d^2/v, σ/d and ΔT respectively. The mass flux at the interface of the bubble is scaled with $k\Delta T/d\mathscr{L}$ where $\mathscr{L}$ is the latent heat of vaporization. Note that the scaling of the pressure differs from that used by Burelbach *et al.* (1988).

The liquid velocity (u, v) where $u = u(x, y, t)$ and $v = v(x, y, t)$, pressure $p = p(x, y, t)$ and temperature $T = T(x, y, t)$ satisfy the continuity and Navier–Stokes equations,

$$u_x + v_y = 0, \tag{1}$$

$$C(u_t + uu_x + vu_y) = -p_x + C(u_{xx} + u_{yy}), \tag{2}$$

$$C(v_t + uv_x + vv_y) = -p_y + C(v_{xx} + v_{yy}), \tag{3}$$

where $C = \mu v/\sigma d$ is the capillary number, and the energy equation

$$P(T_t + uT_x + vT_y) = T_{xx} + T_{yy}, \tag{4}$$

where $P = v/\kappa$ is the Prandtl number and t denotes time.

At the lower plate $y = -1$ there is the no-slip condition on the liquid velocity, $u = v = 0$, and prescribed temperature, $T = T_0$, where $T_0 = 1$ corresponds to superheating and $T_0 = -1$ to subcooling.

At the lower liquid–vapour interface $y = -1 + h(x,t)$ the local mass-balance condition yields

$$-EJ = (h_t + uh_x - v)(1 + h_x^2)^{-1/2}, \tag{5}$$

where $J = J(x,t)$ denotes the mass flux at the interface due to evaporation or condensation and $E = k\Delta T/\rho v \mathscr{L}$ is the non-dimensional evaporation number (the ratio of the viscous timescale d^2/v to the evaporative timescale $\rho d^2 \mathscr{L}/k\Delta T$). Neglecting the kinetic energy of the vapour particles, the local energy-balance condition yields

$$J = (T_x h_x - T_y)(1 + h_x^2)^{-1/2}. \tag{6}$$

The normal-stress condition yields

$$-p + 2C[v_y + h_x^2 u_x - h_x(u_y + v_x)](1 + h_x^2)^{-1} = h_{xx}(1 + h_x^2)^{-3/2} \tag{7}$$

and the tangential-stress condition yields

$$(1 - h_x^2)(u_y + v_x) - 2h_x(u_x - v_y) = 0. \tag{8}$$

The constitutive equation relating the interfacial temperature to the interfacial mass flux, derived from the kinetic theory of non-uniform gases (see, for example, Schrage 1953), has the linearized form

$$KJ = T, \tag{9}$$

where the non-dimensional parameter

$$K = \frac{kT_s^{3/2}}{\hat{\alpha} d \mathscr{L}^2 \rho^{(V)}} \left(\frac{2\pi R_g}{M_w}\right)^{1/2} \tag{10}$$

measures the degree of non-equilibrium at the interface; $\hat{\alpha}$ is the accommodation coefficient, R_g is the universal gas constant and M_w is the molecular weight of the vapour.

Finally, global conservation of mass means that the rate of change of the bubble mass is equal to

$$DE \int J \, \mathrm{d}s, \tag{11}$$

where $D = \rho/\rho^{(V)}$ denotes the ratio of liquid density to vapour density and the integral is over all appropriate parts of the bubble interface, parameterized by the arclength s.

2.1. *Capillary-statics region*

Away from the plates capillary effects dominate the flow. At leading order in C equations (2) and (3) are simply $p_x = p_y = 0$ and the boundary condition (7) yields

$$-\Delta p = h_{xx}(1 + h_x^2)^{-3/2}, \tag{12}$$

where Δp is the unknown (constant) leading-order pressure drop across the bubble interface. Integrating equation (12) for the interface profile yields the circular arc

$$h = 1 - (\Delta p)^{-1}\left[1 - (1 + \Delta p\,(x - R - S))^2\right]^{1/2} \tag{13}$$

satisfying $h(R+S)=1$ and $|h_x|\to\infty$ as $x\to(R+S)^-$. This is exactly the two-dimensional version of the isothermal capillary-statics region obtained by Bretherton (1961).

2.2. *Transition region*

The solution in the capillary-statics region is dominated by capillary effects and fails to describe the solution in the transition region near $x=R(t)$, $y=-1$ in which viscous effects become important. In order to determine the correct leading-order behaviour in this region one must rescale the variables appropriately. Since the solution must match with that in the capillary-statics region and capillary forces must be balanced by viscous forces due to the relative motion of the transition region and the lower plate one must rescale $x-R$ with $C^{1/3}$, $y+1$ with $C^{2/3}$, v with $C^{1/3}$ and h with $C^{2/3}$. Thus new variables defined by $x=R+C^{1/3}\hat{x}$, $y=-1+C^{2/3}\hat{y}$, $v=C^{1/3}\hat{v}$ and $h=C^{2/3}\hat{h}$ are introduced. Note that this choice of scale means that the transition region will be thin, and so the governing equations will be of lubrication type. A non-trivial leading-order balance can be retained in equations (6) and (9) only if $J=O(C^{-2/3})$ and $K=O(C^{2/3})$ and so one writes $J=C^{-2/3}\hat{J}$ and $K=C^{2/3}\hat{K}$ where $\hat{J}$ and $\hat{K}$ are both $O(1)$ in the limit $C\to 0$.

At leading order in C equations (1)–(4) yield the familiar lubrication equations

$$u_{\hat{x}}+\hat{v}_{\hat{y}}=0, \tag{14}$$

$$u_{\hat{y}\hat{y}}=p_{\hat{x}}, \tag{15}$$

$$0=p_{\hat{y}}, \tag{16}$$

$$T_{\hat{y}\hat{y}}=0, \tag{17}$$

while the boundary conditions at the bubble interface $\hat{y}=\hat{h}(\hat{x},t)$ (5)–(9) yield

$$-EC^{-1}\hat{J}=u\hat{h}_{\hat{x}}-\hat{v}, \tag{18}$$

$$\hat{J}=-T_{\hat{y}}, \tag{19}$$

$$-p=\hat{h}_{\hat{x}\hat{x}}, \tag{20}$$

$$u_{\hat{y}}=0, \tag{21}$$

$$\hat{K}\hat{J}=T, \tag{22}$$

and the boundary conditions on the plate $\hat{y}=0$ yield $u=-U$ and $\hat{v}=0$, where $U=U(t)=R_t>0$ is the velocity of the transition region, and $T=T_0$. Note that when $U<0$ the retreating transition region 'sweeps up' the liquid (if any) on the plate and the details of the flow in the transition region are unimportant.

If $E=o(C)$ then the solution for the leading-order problem for the velocity, pressure and interface profile is independent of mass-transfer effects, and so can be solved in the usual way to obtain

$$3U\hat{h}_{\hat{x}}=(\hat{h}^3\hat{h}_{\hat{x}\hat{x}\hat{x}})_{\hat{x}}. \tag{23}$$

Evidently equation (23) has the uniform solution $\hat{h}=\hat{h}_\infty$ for all values of the constant $\hat{h}_\infty$ and can be integrated once with respect to $\hat{x}$ to obtain the appropriate version of the well-known Landau–Levich equation for the interface profile,

$$\hat{h}_{\hat{x}\hat{x}\hat{x}}=3U\frac{(\hat{h}-\hat{h}_\infty)}{\hat{h}^3}. \tag{24}$$

This equation was first obtained by Landau & Levich (1942) and is perhaps the best

known of a large class of nonlinear third-order differential equations which arise in the study of thin films with surface tension (see the review articles by Tuck & Schwartz 1990 and Myers 1998 for further details). Writing $\hat{x} = (3U)^{-1/3}\hat{h}_\infty X$ and $\hat{h} = \hat{h}_\infty H$, one obtains the canonical form of equation (24), namely

$$H_{XXX} = \frac{H-1}{H^3}. \tag{25}$$

No analytical solution has been obtained to this equation but, as Bretherton (1961) described, it has the appropriate asymptotic solutions $H \sim 1$ as $X \to -\infty$ and

$$H \sim C_0\frac{X^2}{2} + C_1X + C_2 \tag{26}$$

as $X \to \infty$, where C_0, C_1 and C_2 are undetermined constants.† This latter solution will only match with the solution in the capillary-statics region given by equation (13) if $S = 1$ and $\Delta p = 1$, i.e. only if the bubble interface in the capillary-statics region is (at leading order) a semicircular 'cap' which fits exactly between the plates. This matching procedure also determines that $\hat{h}_\infty = (3U)^{2/3}C_0$ where the value of the constant $C_0 = 0.6429$ is easily calculated numerically, and so

$$\hat{h}_\infty = c\,U^{2/3}, \tag{27}$$

where $c = 1.337$. See Park & Homsy (1984) and Wilson (1995) for details of the matching procedure. In the special case $U = 1$ one recovers the familiar steady transition region described by Landau & Levich (1942) and Bretherton (1961).

2.3. *Thin-film region*

When $U > 0$ the solution in the transition region produces a quiescent film of liquid on the plate whose height depends on the speed with which the transition region is moving as it is deposited according to equation (27). In the steady, isothermal problem studied by Bretherton (1961) this film is of uniform thickness and so requires no further attention. However, in the present problem the situation is significantly more complicated. Since the motion is unsteady, the thin film will not now be deposited with constant thickness. Furthermore, the superheating or subcooling of the plates will cause the profile of the thin film to vary once it has been deposited and may even cause the film to dry out locally at various places and times on a superheated plate, possibly causing the thin film to break up into disconnected patches of liquid as it dries. In order to determine the correct leading-order behaviour in this thin-film region one must again rescale the variables appropriately. Since the solution must match with that in the transition region one must rescale $y + 1$ with $C^{2/3}$, v with $C^{2/3}$ and h with $C^{2/3}$. Note, however, that there is now no reason to rescale x and that as a consequence the scale for v differs from that used in the transition region. Thus new variables defined by $y = -1 + C^{2/3}\bar{y}$, $v = C^{2/3}\bar{v}$ and $h = C^{2/3}\bar{h}$ are introduced. Note that the thin-film region is much longer than the transition region and so the governing equations will again be of lubrication type.

At leading order in C equations (1)–(4) yield the simplified lubrication equations

$$u_x + \bar{v}_{\bar{y}} = 0, \tag{28}$$

$$u_{\bar{y}\bar{y}} = 0, \tag{29}$$

† Duffy & Wilson (1997) describe in detail the exact solution of the equation $H_{XXX} = H^{-2}$ satisfied by the solutions of equation (25) in the limit $|H| \to \infty$.

$$0 = p_{\bar{y}}, \tag{30}$$

$$T_{\bar{y}\bar{y}} = 0, \tag{31}$$

while the boundary conditions at the bubble interface $\bar{y} = \bar{h}(x,t)$ (5)–(9) yield

$$-EC^{-4/3}\hat{J} = \bar{h}_t + u\bar{h}_x - \bar{v}, \tag{32}$$

$$\hat{J} = -T_{\bar{y}}, \tag{33}$$

$$p = 0, \tag{34}$$

$$u_{\bar{y}} = 0, \tag{35}$$

$$\hat{K}\hat{J} = T, \tag{36}$$

and the boundary conditions on the plate $\bar{y} = 0$ yield $u = \bar{v} = 0$ and $T = T_0$.

This problem can be solved immediately to yield $u = \bar{v} = 0$ (i.e. the film is quiescent as expected) together with

$$T = T_0\left[1 - \frac{\bar{y}}{\hat{K} + \bar{h}}\right], \quad \hat{J} = \frac{T_0}{\hat{K} + \bar{h}}. \tag{37}$$

If $E = O(C^{4/3})$ then mass-transfer effects enter the equation for the interface profile at leading order and so if one writes $E = \hat{E}C^{4/3}$ where $\hat{E}$ is $O(1)$ in the limit $C \to 0$, then equation (32) yields

$$\bar{h}_t + \frac{\hat{E}T_0}{\hat{K} + \bar{h}} = 0. \tag{38}$$

Note that this choice of E is consistent with the restriction $E = o(C)$ used to obtain the solution in the transition region in § 2.2. Equation (38) is exactly the equation describing the evolution of an evaporating or condensing liquid film of uniform thickness on a superheated or subcooled plate first derived by Burelbach *et al.* (1988).

2.4. *Global mass-conservation condition*

Now that the leading-order problems have been obtained in all three regions, the next step is to evaluate the leading-order version of the global mass-conservation condition (11). In the capillary-statics region $J = O(1)$ and $s = O(1)$ and so the contribution to the integral in (11) is $O(1)$; in the transition region $J = O(C^{-2/3})$ but $s = O(C^{1/3})$ and so the contribution is $O(C^{-1/3})$; in the thin-film region $J = O(C^{-2/3})$ and $s = O(1)$ and so the contribution is $O(C^{-2/3})$. Hence the mass transfer is dominated by that in the thin-film region and the leading-order version of (11) is simply

$$DE\int J\,\mathrm{d}x, \tag{39}$$

where the integral is over appropriate parts of the interval $[0, R]$, specifically over all $[0, R]$ for condensation but only over those parts of $[0, R]$ covered by liquid (i.e. with $h > 0$) for evaporation. Since at leading order the rate of change of mass of the bubble is simply equal to $R_t = U$, one obtains a non-trivial leading-order global mass-conservation condition only if $D = O(C^{-2/3})$ and so one writes $D = \hat{D}C^{-2/3}$ where $\hat{D}$ is $O(1)$ in the limit $C \to 0$. Notice that since $D \gg 1$ this choice is consistent with the one-sided model. Thus, using equation (37) the leading-order global mass-conservation condition can be written as

$$U = \hat{D}\hat{E}\int \frac{T_0}{\hat{K} + \bar{h}}\,\mathrm{d}x. \tag{40}$$

2.5. *Problem summary*

In order to calculate the dynamics of the bubble expansion or contraction one has to solve equation (38) for the profile of the liquid film in the thin-film region subject to the boundary condition (27) at $x = R(t)$; the solution for $U(t)$ is then calculated by solving the global mass-conservation condition (40). The remainder of this paper is devoted to an analysis of this problem for different initial conditions defined on $x \in [0, L]$ at $t = 0$ where $L = R(0) > 0$.

For simplicity of presentation it is useful to introduce rescaled variables $\bar{y} = cy^*$, $\bar{h} = ch^*$, $\hat{K} = cK^*$, $\hat{E}T_0 = c^2E^*K^*$ and $\hat{D} = c^{-1}D^*$. Dropping the asterisks immediately for clarity, equation (38) for the profile of the thin film $h = h(x, t)$ becomes

$$h_t + \frac{E}{1 + \alpha h} = 0, \tag{41}$$

subject to the boundary condition

$$h = U^{2/3} \tag{42}$$

at $x = R(t)$ and the global mass-conservation condition

$$U(t) = DE \int \frac{\mathrm{d}x}{1 + \alpha h(x, t)}, \tag{43}$$

where $\alpha \equiv 1/K$. The boundary condition (42) plays a central role as it determines the thickness of the thin film as it is deposited in terms of the instantaneous speed of the transition region. When $\alpha = 0$ one recovers the special case in which the mass flux at the interface is independent of h and in this case the solution for $U(t)$ depends only on the length of the regions covered by liquid and not the thickness of the film in those regions.

Equation (41) can be immediately solved to yield

$$h(x, t) = -\frac{1}{\alpha} + \left[\left(\frac{1}{\alpha} + h_0(x)\right)^2 - \frac{2E}{\alpha}(t - t_0(x))\right]^{1/2}, \tag{44}$$

and so equation (43) yields

$$U(t) = DE \int [(1 + \alpha h_0(x))^2 - 2\alpha E(t - t_0(x))]^{-1/2}\, \mathrm{d}x. \tag{45}$$

If $x < L = R(0)$, then $h_0 = h_0(x)$ is the initial profile of the thin film at $t = t_0 = 0$, while if $x > L$, then h_0 denotes the thickness of the liquid film deposited at position x at time $t = t_0(x) = R^{-1}(x)$.

Note that when the plate is superheated, $E > 0$, then the liquid evaporates from the thin film and the film dries out locally at position x at time t given by

$$t - t_0(x) = \frac{h_0(x)}{E}\left(1 + \frac{\alpha h_0(x)}{2}\right). \tag{46}$$

However, if the plate is subcooled, $E < 0$, then vapour condenses onto the thin film and local dry-out never occurs.

3. Delay-equation formulation for a continuous film

There is, in general, no reason to expect that the liquid in the thin film will remain as a single, continuous film as it dries (indeed, it will become apparent that typically

it does not). However, it is informative to consider the solution in this special case before analysing the more general situation. In this case write $t = \tau + \mathscr{T}(\tau)$ and denote the position of the front of the film (where it is being deposited) by $x = R(\tau + \mathscr{T}(\tau))$ and the back (where $h = 0$) by $x = R(\tau)$. The delay $\mathscr{T} = \mathscr{T}(\tau)$ represents the length of time it takes for the liquid deposited at $x = R(\tau)$ at time $t = \tau$ to dry out, and hence from equation (46) is given by

$$\mathscr{T}(\tau) = \frac{1}{2\alpha E}\left[\left(1 + \alpha U(\tau)^{2/3}\right)^2 - 1\right]. \tag{47}$$

By changing the variable of integration, equation (45) can be expressed in the form

$$U(\tau + \mathscr{T}(\tau)) = DE \int_{\tau}^{\tau+\mathscr{T}(\tau)} U(\hat{\tau})\,[1 + f(\hat{\tau}) - f(\tau)]^{-1/2}\ \mathrm{d}\hat{\tau}, \tag{48}$$

where

$$f(\tau) = \left(1 + \alpha U(\tau)^{2/3}\right)^2 + 2\alpha E\tau. \tag{49}$$

Equation (48) is an integro-delay equation for U with a non-constant delay $\mathscr{T}(\tau)$ which depends on the solution according to equation (47). Unfortunately the general solution to this equation is not available, even in the case $\alpha = 0$ in which equation (47) reduces to

$$\mathscr{T}(\tau) = E^{-1}U(\tau)^{2/3} \tag{50}$$

and equation (48) takes the particularly simple form

$$U(\tau + \mathscr{T}(\tau)) = DE\,[R(\tau + \mathscr{T}(\tau)) - R(\tau)]\,. \tag{51}$$

However, as described in the next section, useful progress can still be made with this delay-equation formulation of the problem.

4. Constant-velocity solution

Equation (48) permits an exact, steady travelling-wave solution in which U and $\mathscr{T}$ are constant. Substituting $U = U_0$ (a constant) into equation (48) yields the single non-trivial solution

$$U_0 = D^{-3/2} \tag{52}$$

and hence from equation (47)

$$\mathscr{T} = \mathscr{T}_0 = E^{-1}D^{-1}\left(1 + \frac{\alpha}{2D}\right) \tag{53}$$

and from equation (44)

$$h = h_0 = -\frac{1}{\alpha} + \left[\left(\frac{1}{\alpha} + \frac{1}{D}\right)^2 - \frac{2E}{\alpha}(t - D^{3/2}x)\right]^{1/2}, \tag{54}$$

valid between the back

$$x = R(t - \mathscr{T}) = D^{-3/2}(t - \mathscr{T}) = D^{-3/2}t - E^{-1}D^{-5/2}\left(1 + \frac{\alpha}{2D}\right) \tag{55}$$

and the front $x = R(t) = D^{-3/2}t$ of the film. The profile of the film according to equation (54) at $t = 0$ is shown in figure 2 for a range of values of α in the case $D = E = 1$. In particular, figure 2 shows that all the profiles satisfy $h(R(t), t) = D^{-1}$ at the front and have contact angle $ED^{3/2}$ at the back.

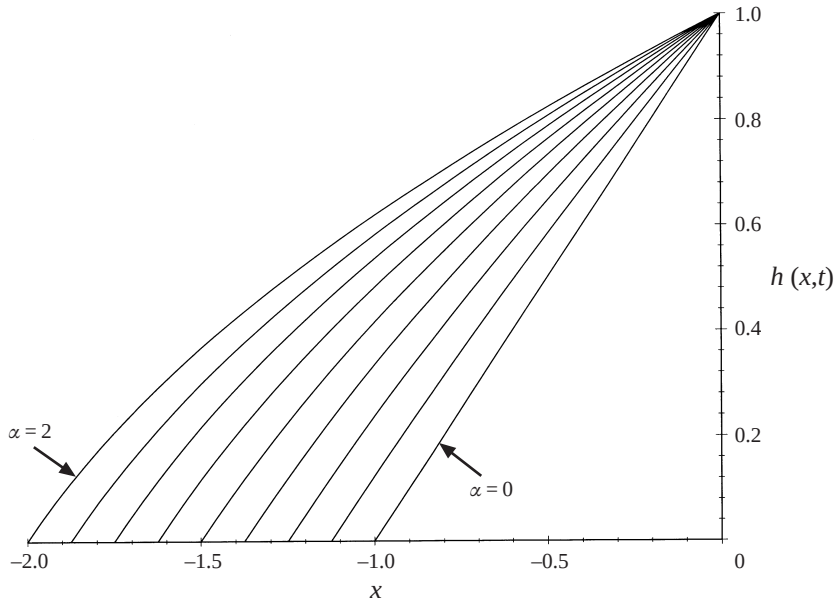

FIGURE 2. Thin-film profiles of the constant-velocity solutions given by equation (54) at $t = 0$ for $\alpha = 0, 0.25, 0.5, \ldots, 2$ in the case $D = E = 1$. Note that all the profiles move to the right with the same speed, $U_0 = D^{-3/2}$.

One can investigate the linear stability of this constant-velocity solution by writing $U = U_0 + U_1$ and $\mathscr{T} = \mathscr{T}_0 + \mathscr{T}_1$ and linearizing for small U_1 and $\mathscr{T}_1$ to obtain the first-order delay $\mathscr{T}_1(\tau)$ from equation (47),

$$\mathscr{T}_1(\tau) = \frac{2}{3EU_0^{1/3}}(1 + \alpha U_0^{2/3})U_1(\tau), \tag{56}$$

and the equation for $U_1(\tau)$ from equation (48),

$$U_1(\tau + \mathscr{T}_0) = \frac{2D}{3U_0^{1/3}}U_1(\tau) + DE\int_\tau^{\tau+\mathscr{T}_0} U_1(\hat{\tau})\,[1 + 2\alpha E(\hat{\tau} - \tau)]^{-1/2}\ \mathrm{d}\hat{\tau}$$
$$-\frac{2\alpha DE}{3}U_0^{2/3}(1 + \alpha U_0^{2/3})\int_\tau^{\tau+\mathscr{T}_0} [U_1(\hat{\tau}) - U_1(\tau)]\,[1 + 2\alpha E(\hat{\tau} - \tau)]^{-3/2}\ \mathrm{d}\hat{\tau}. \tag{57}$$

Equation (57) is a integro-delay equation for U_1 with constant (known) delay $\mathscr{T}_0$ which has the exact exponential solution

$$U_1(\tau) = A\exp(E\beta\tau), \tag{58}$$

where A is an arbitrary constant and β satisfies a complicated nonlinear equation involving D (but not E), which is not reproduced here for brevity. In the limit $\alpha \to 0$ this equation simplifies to

$$\frac{\beta}{D}\left[\exp\left(\frac{\beta}{D}\right) - \frac{2D^{3/2}}{3}\right] - \exp\left(\frac{\beta}{D}\right) + 1 = 0. \tag{59}$$

Numerically calculated solutions for β as a function of α for a range of values of D in figure 3 show that $\beta > 0$ for all α for all the values of D investigated, i.e. the uniform velocity solution is *unconditionally unstable*. Specifically, the numerical calculations

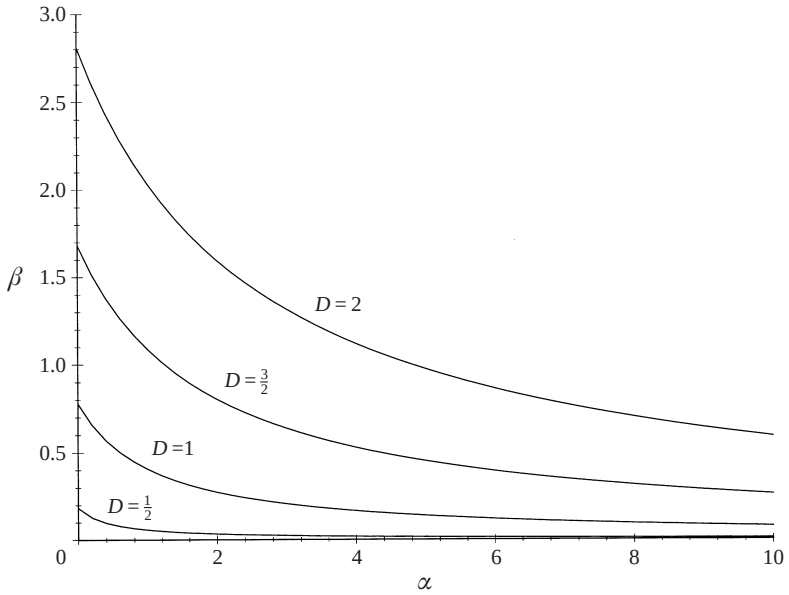

FIGURE 3. Numerically calculated solutions for the temporal growth rate β of the constant-velocity solutions plotted as a function of α for $D = 0.5, 1, 1.5, 2$.

show that β is a positive, monotonically decreasing function of α which approaches the solution of equation (59) in the limit $\alpha \to 0$ (and so, for example, in this limit $\beta = 0.004102$ when $D = 10^{-1}$, $\beta = 0.779926$ when $D = 1$ and $\beta = 33.845134$ when $D = 10$) and satisfies $\beta = O(\alpha^{-1})$ in the limit $\alpha \to \infty$.

5. Numerical solution

In general one has to resort to numerical techniques in order to solve equation (45).

The solution for $U(t)$ at $t = n\Delta t$ for $n = 0, 1, 2, \ldots$ (where $\Delta t > 0$ is the constant time step) is approximated by U^n and the corresponding approximation to $R(t)$, R^n, is obtained from the U^n by simple quadrature using the trapezoidal rule. Starting from the known initial conditions at $N = 0$, the solution at each new timestep $N + 1$ is calculated explicitly in terms of the known solutions at timesteps $0, 1, 2, \ldots, N$ as follows. First, the new thin-film profile is calculated at each spatial grid-point R^n for $n = 0, 1, \ldots, N$ using equation (44). Then, the integral in equation (45) is evaluated using the trapezoidal rule over those sub-intervals of the interval $[0, R^{N+1}]$ in which $h > 0$, resulting in a nonlinear equation for U_{N+1} which is solved numerically using Newton's method. This process is repeated until the solution is obtained over the desired time interval. Particular care is required when the solution for $U(t)$ has discontinuities (as it has for the uniform initial profile discussed subsequently) and in this case an extra timestep of zero length is included to capture the solution at $t = t_c^+$ (just after the discontinuity) as well as at $t = t_c^-$ (just before the discontinuity). In practice in order to increase the accuracy of the procedure the contribution to the integral in equation (45) from the interval $[0, L]$ due to the initial profile is calculated analytically rather than numerically. This explicit numerical procedure could be generalized to an implicit one, but this is not found to be necessary for the present purposes.

The entire procedure is implemented numerically using the MAPLE V computer algebra package running on a SiliconGraphics INDIGO^2 workstation in the Department of Engineering Sciences and Applied Mathematics at Northwestern University. Depending on the size of the timestep and the range of t required, the calculations described subsequently take anything from a few seconds to a couple of hours of CPU time to complete. The accuracy of the solution is then checked by repeating the procedure with smaller timesteps until the solution has converged to the desired accuracy. Depending on the size of L, the solutions depicted subsequently are typically obtained with a timestep of between 0.1 and 0.01 and the solutions are converged to better than 5%. The accuracy of the solution at the first few timesteps is verified by comparison with the asymptotic solution in the limit $t \to 0$.

In a real boiling situation the 'initial' profile of the thin film would be determined by the details of the bubble nucleation process, a subject beyond the scope of the present work. In what follows the evolution of the thin film will be investigated starting from two simple initial profiles defined on $[0, L]$ with thickness H at $x = L$, namely a *uniform* initial film $h = H$ and a *linear* initial film $h = Hx/L$. In all the numerical computations which follow $H = 1$ and $D = 1$.

6. Problem 1: both plates superheated

If both plates are superheated then $E > 0$ and the liquid in the thin films will evaporate causing the bubble to expand, i.e. $U(t) \geqslant 0$.

6.1. *Uniform initial film*

For the uniform initial film the contribution to the integral in equation (45) from the initial profile is given simply by

$$DEL\left[(1+\alpha H)^2 - 2\alpha E t\right]^{-1/2} \tag{60}$$

for $t \in [0, t_c]$ where from equation (46)

$$t_c = \frac{H}{E}\left(1 + \frac{\alpha H}{2}\right), \tag{61}$$

and the initial behaviour of $U(t)$ is given by $U = U_0 + U_1 t + O(t^2)$ where

$$U_0 = \frac{DEL}{1+\alpha H} > 0, \quad U_1 = \frac{DEU_0}{1+\alpha U_0^{2/3}} + \frac{\alpha D E^2 L}{(1+\alpha H)^3}. \tag{62}$$

Typical numerically calculated solutions for $U(t)$ are shown in figure 4(a) for a range of values of L in the case $E = \alpha = 1$. Figure 4(a) clearly demonstrates that the solutions for $U(t)$ are typically not monotonic and shows the delay character of the system evidenced by the 'echoes' in the solutions for $U(t)$. The corresponding thin-film profiles at several different times in the case $L = 1$ and $L = 0.75$ are shown in figure 4(b) and figure 4(c) respectively. In particular, note that figure 4(c) shows that in the case $L = 0.75$ the thin film becomes discontinuous at $t = 1$ and again at $t = 3$, but is continuous at the other times shown, namely $t = 0, 2, 4, 5$.

As figure 4(a) shows, U initially increases until the disappearance of the initial film and the consequent discontinuous drop of magnitude DEL in the mass flux to the bubble at $t = t_c$ causes it to drop as well. Note that in the special case $\alpha = 0$ this initial increase is given by simply $U = DEL\exp(DEt)$ and the effect of increasing α from zero is to reduce U from this value and to increase t_c. Apart from the discontinuity at $t = t_c$

the solutions for U are otherwise continuous but not smooth. The 'corners' in the graph of $U(t)$ result from the local dry-out of film which causes the local mass flux to drop discontinuously. For example, the thin film breaks at $x = L$ before the initial film dries out at $t = t_c$ if the thickness of the film deposited at $x = L$ at $t = 0$ is less than H, i.e. if $DEL < H^{3/2}(1+\alpha H)$. This condition is satisfied by all the solutions shown in figure 4 except that corresponding to $L = 2$ and the effect of this local dry-out can be seen in the weak slope discontinuities which occur before $t = t_c$ in each of the other solutions for U. The thin-film profiles in the case $L = 0.75$ shown in figure 4(c) confirm that in this case the thin film does indeed dry out locally near $x = L$ at $t = 1 < t_c = 3/2$.

Perhaps the most striking feature of the solutions shown in figure 4(a) is that the ultimate fate of the bubble depends critically on the details of the initial conditions, specifically if $L < L_c$ then $U \to 0$ at $t = t_m$ (say), and so the expansion of the bubble stops in a finite time, while if $L > L_c$ then $U \to \infty$ as $t \to \infty$, and so the bubble continues to expand for all time. Numerical determination of the exact value of L_c is difficult because small errors in the solution at the early timesteps can have a dramatic effect of the large-time behaviour of $U(t)$ when L is near its critical value, but from the results shown in figure 4(a) evidently $L_c \in (0.91, 0.92)$ when $E = \alpha = 1$. Numerically calculated values of t_m are plotted as a function of L in figure 5 for a range of values of E and α. Figure 5 shows the expected vertical asymptotes in t_m at $L = L_c$ and indicates that the effect of increasing α and E simultaneously (which corresponds to decreasing the non-equilibrium parameter K) is to decrease t_m for small L and to decrease L_c.

6.2. *Linear initial film*

For the linear initial film the contribution to the integral in equation (45) from the initial profile is given by

$$\frac{DEL}{\alpha H} \log \left[\frac{1 + \alpha H + \left[(1+\alpha H)^2 - 2\alpha E t\right]^{1/2}}{1 + (1 + 2\alpha E t)^{1/2}} \right], \tag{63}$$

and the initial behaviour of $U(t)$ is given by $U = U_0 + U_1 t + O(t^2)$ where

$$U_0 = \frac{DEL}{\alpha H} \log(1 + \alpha H) > 0,$$
$$U_1 = \frac{DEU_0}{1 + \alpha U_0^{2/3}} - \frac{DE^2 L \left[1 + (1+\alpha H)^2\right]}{2H(1+\alpha H)^2}. \tag{64}$$

Typical numerically calculated solutions for $U(t)$ are shown in figure 6(a) for a range of values of L in the case $E = \alpha = 1$. The corresponding thin-film profiles at several different times in the cases $L = 2$ and $L = 1.6$ are shown in figure 6(b) and figure 6(c) respectively. Evidently in this case there are no discontinuities in $U(t)$, but all the other features of the solutions (including the existence of a critical value of L) are qualitatively the same as for a uniform initial film.

7. Problem 2: both plates subcooled

If both plates are subcooled then $E = -C < 0$ and the vapour will condense onto the thin films causing the bubble to contract, i.e. $U(t) \leqslant 0$. This purely condensing case is considerably easier to analyse than the purely evaporating case considered in § 6 for two reasons. First, because the vapour is condensing onto the thin film the film always remains continuous (i.e. no dry patches form) and secondly, because the

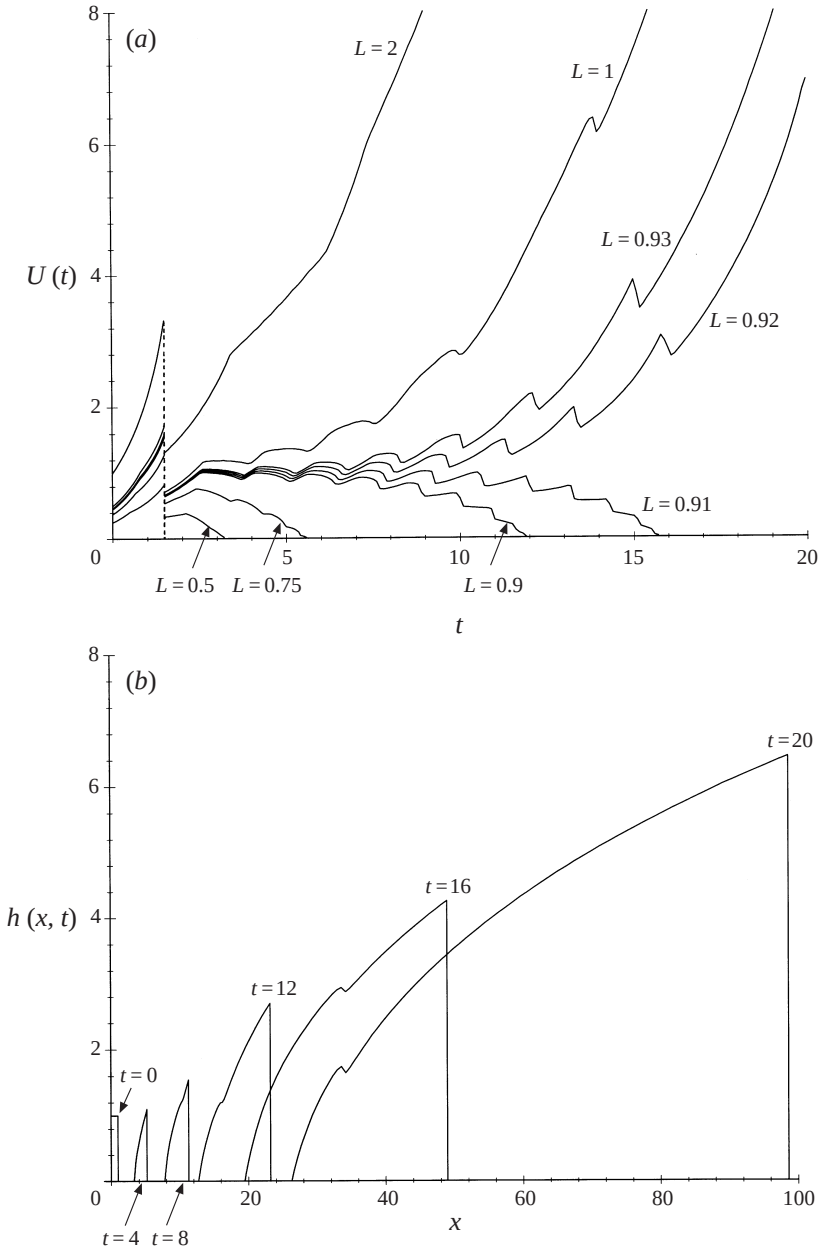

FIGURE 4(*a*, *b*). For caption see facing page.

bubble is contracting the condensation only takes place onto the initial film and so the integrand in equation (45) is known explicitly.

7.1. *Uniform initial film*

For the uniform initial film equation (45) can easily be solved exactly to yield

$$U = -\frac{DCL}{g(t)} \exp\left[-\frac{D}{\alpha}\left(g(t) - g(0)\right)\right], \tag{65}$$

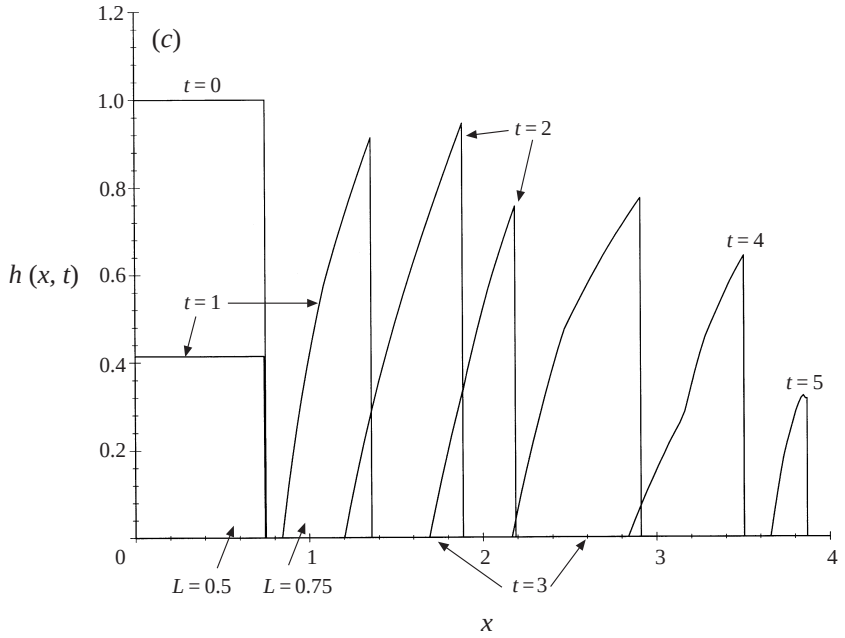

FIGURE 4. (*a*) Numerically calculated solutions for $U(t)$ for a uniform initial film in the case $E = \alpha = 1$ when both plates are superheated for $L = 0.5, 0.75, 0.9, 0.91, 0.92, 0.93, 1, 2$; (*b*) the corresponding thin-film profiles at $t = 0, 4, 8, 12, 16, 20$ in the case $L = 1 > L_c$; and (*c*) the corresponding thin film profiles at $t = 0, 1, 2, 3, 4, 5$ in the case $L = 0.75 < L_c$. Note that in (*c*) the thin film is discontinuous at $t = 1$ and $t = 3$, but is continuous at the other times shown.

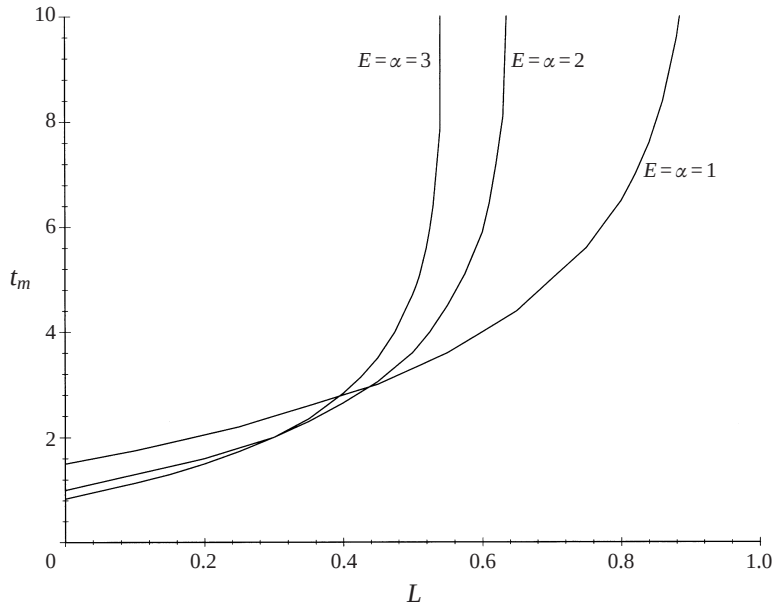

FIGURE 5. Numerically calculated values of t_m plotted as a function of L for $E = \alpha = 1, 2, 3$.

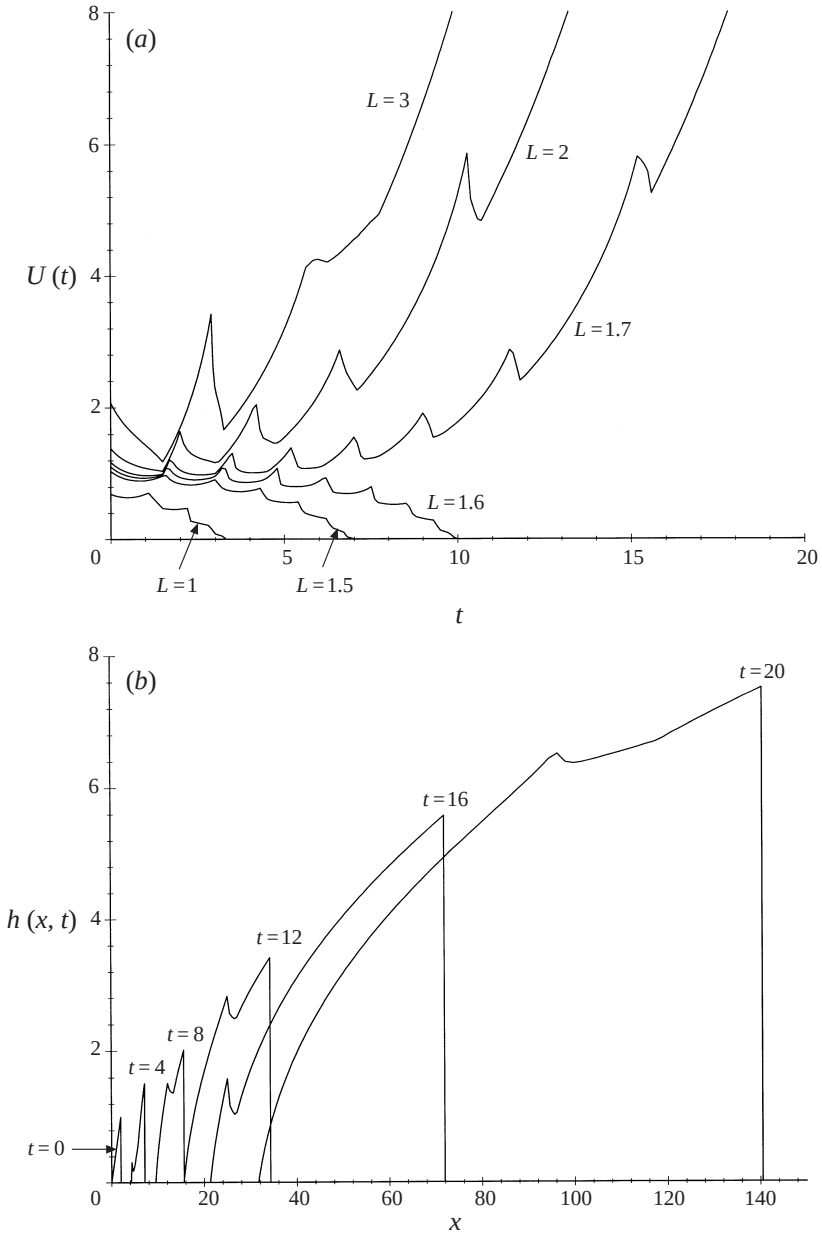

FIGURE 6(*a*, *b*). For caption see facing page.

where

$$g(t) = \left[(1+\alpha H)^2 + 2\alpha C t\right]^{1/2}. \tag{66}$$

In particular, the initial behaviour of $U(t)$ is given by $U = U_0 + U_1 t + O(t^2)$ where

$$U_0 = -\frac{DCL}{1+\alpha H} < 0, \quad U_1 = \frac{DC}{(1+\alpha H)^3}\left[\alpha CL - (1+\alpha H)^2 U_0\right]. \tag{67}$$

The solution for $U(t)$ is plotted in figure 7(*a*) for different values of L in the case $C = \alpha = 1$. Typical thin-film profiles (which remain uniform) at several different

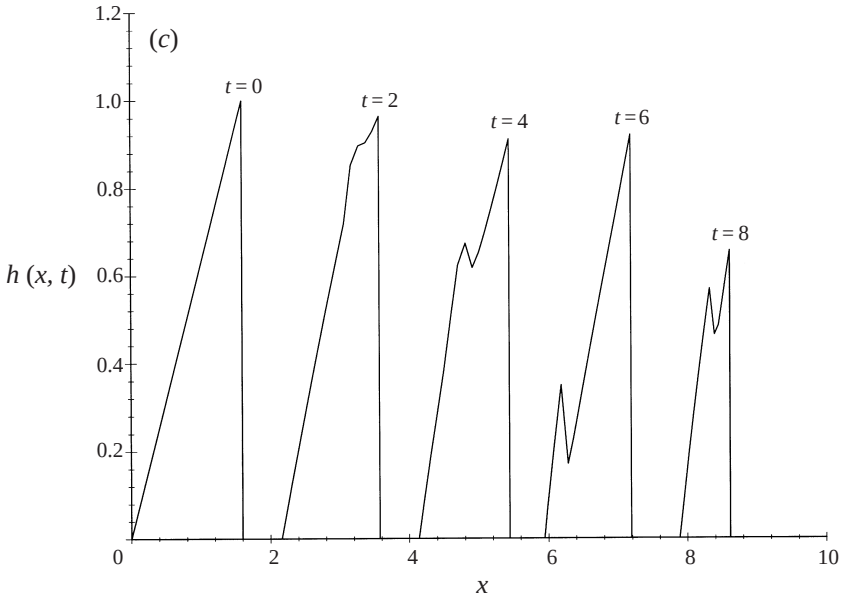

FIGURE 6. (*a*) Numerically calculated solutions for $U(t)$ for a linear initial film in the case $E = \alpha = 1$ when both plates are superheated for $L = 1,\ 1.5,\ 1.6,\ 1.7,\ 2,\ 3$; (*b*) the corresponding thin-film profiles at $t = 0, 4, 8, 12, 16, 20$ in the case $L = 2 > L_c$; and (*c*) the corresponding thin film profiles at $t = 0, 2, 4, 6, 8$ in the case $L = 1.6 < L_c$.

times in the case $L = 1$ are shown in figure 7(*b*). Evidently, U is always negative and increases monotonically from U_0 at $t = 0$ to zero from below and the length of the thin-film region approaches zero asymptotically in the limit $t \to \infty$.

7.2. *Linear initial film*

For the linear initial film equation (45) cannot be solved exactly, but can easily be integrated numerically. The initial behaviour of $U(t)$ is given by $U = U_0 + U_1 t + O(t^2)$ where

$$U_0 = -\frac{DCL}{\alpha H}\log(1+\alpha H) < 0,$$
$$U_1 = \frac{DC}{2(1+\alpha H)^2}\left[\alpha CL(2+\alpha H) - 2(1+\alpha H)U_0\right]. \tag{68}$$

Numerically calculated solutions for $U(t)$ are plotted in figure 8(*a*) for different values of L in the case $C = \alpha = 1$. Typical thin-film profiles at several different times in the case $L = 1$ are shown in figure 8(*b*). Evidently the behaviour in this case is again qualitatively similar to that in the case of a uniform initial film.

8. Problem 3: lower plate superheated and upper plate subcooled

If the lower plate is superheated and the upper plate is subcooled equally then both evaporation and condensation occur and the bubble may either expand or contract.

8.1. *Uniform initial film*

For a uniform initial film on both plates the contribution to the integral in equation (45) from the initial profile is given by

$$\tfrac{1}{2}DEL\left[(1+\alpha H)^2 - 2\alpha Et\right]^{-1/2} - \tfrac{1}{2}DEL\left[(1+\alpha H)^2 + 2\alpha Et\right]^{-1/2}, \tag{69}$$

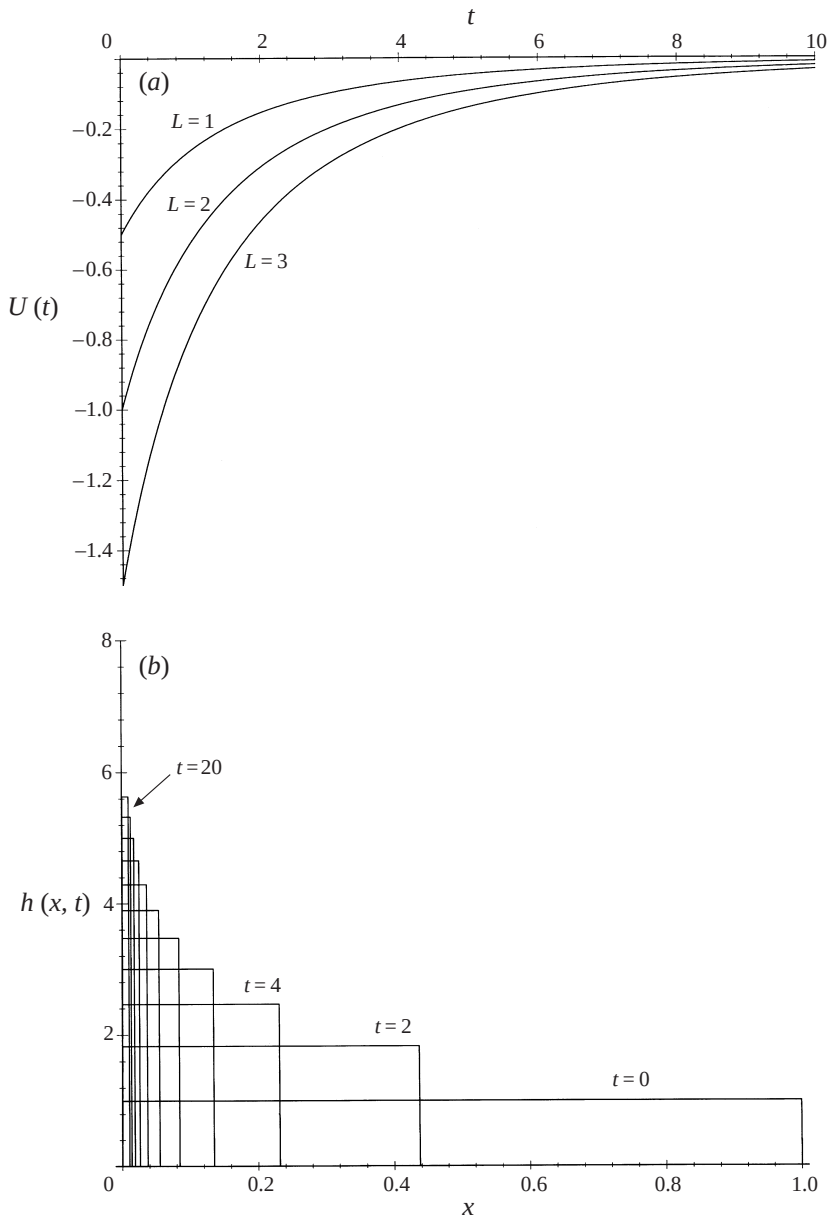

FIGURE 7. (*a*) Solutions for $U(t)$ for a uniform initial film in the case $C = \alpha = 1$ when both plates are subcooled for $L = 1, 2, 3$; (*b*) the corresponding thin-film profiles at $t = 0, 2, 4, \ldots, 20$ in the case $L = 1$.

where the first term is only present for $t \in [0, t_c]$, and the initial behaviour of $U(t)$ is given by $U = U_0 + U_1 t + O(t^2)$ where $U_0 = 0$ and

$$U_1 = \frac{\alpha D E^2 L}{(1 + \alpha H)^3} > 0. \tag{70}$$

Typical numerically calculated solutions for $U(t)$ are shown in figure 9(*a*) for a range of values of L in the case $E = \alpha = 1$. The corresponding thin-film profiles on both

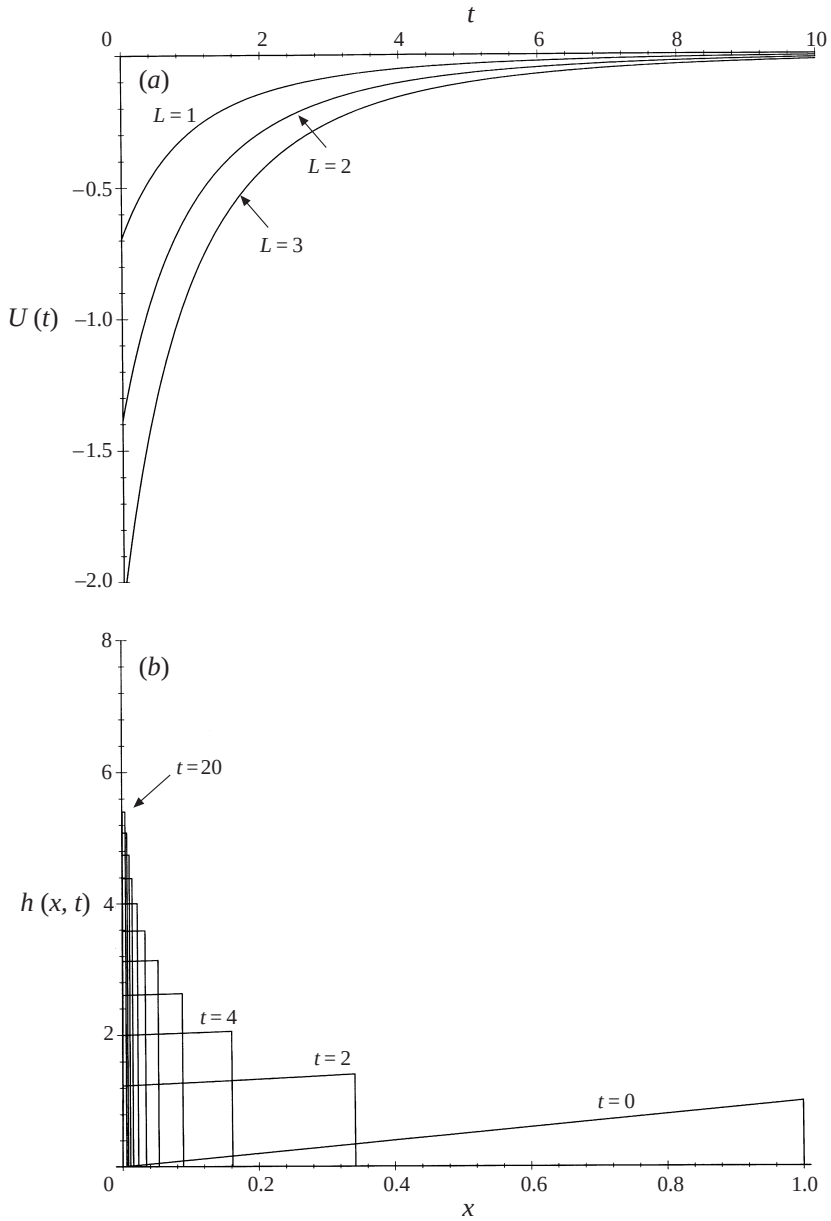

FIGURE 8. (*a*) Numerically calculated solutions for $U(t)$ for a linear initial film in the case $C = \alpha = 1$ when both plates are subcooled for $L = 1, 2, 3$; (*b*) the corresponding thin-film profiles at $t = 0, 2, 4, \ldots, 20$ in the case $L = 1$.

plates at several different times in the case $L = 1$ are shown in figure 9(*b*) and figure 9(*c*) respectively.

Initially evaporation effects are dominant and the bubble expands ($U > 0$) until $t = t_c$ when the disappearance of the initial film on the superheated plate causes a discontinuous drop of magnitude $DEL/2$ in the mass flux to the bubble, and hence a discontinuous drop in U as well. Thereafter, condensation effects are dominant and the bubble contracts ($U < 0$). Eventually the remaining liquid on the superheated plate will either have evaporated or have been swept up by the retreating transition

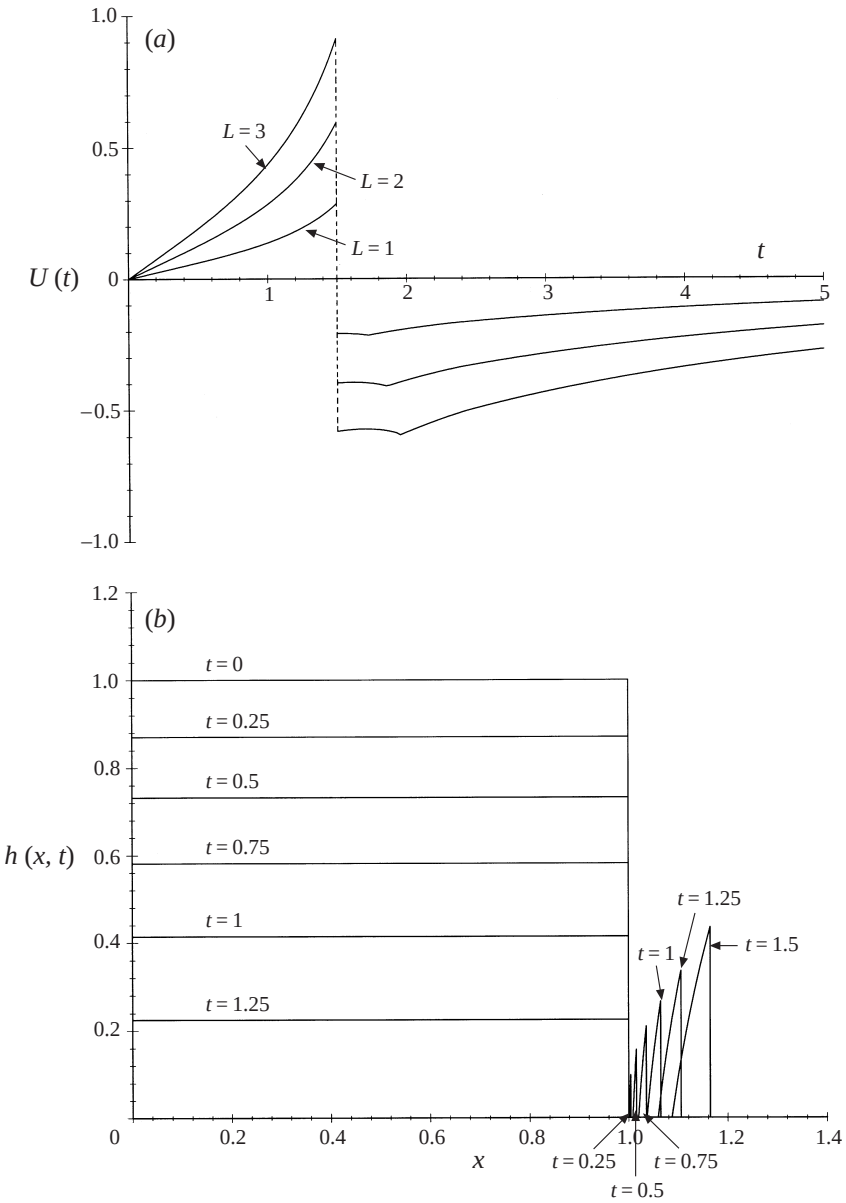

FIGURE 9 (*a*, *b*). For caption see facing page.

region. Thereafter, only condensation occurs and so, as in the pure-condensation case considered earlier, U approaches zero from below and the length of the thin-film region approaches zero asymptotically in the limit $t \to \infty$.

8.2. *Linear initial film*

For a linear initial film on both plates the initial behaviour of $U(t)$ is given by $U = U_0 + U_1 t + O(t^2)$ where $U_0 = 0$ and

$$U_1 = -\frac{DE^2L}{2H(1+\alpha H)^2} < 0. \tag{71}$$

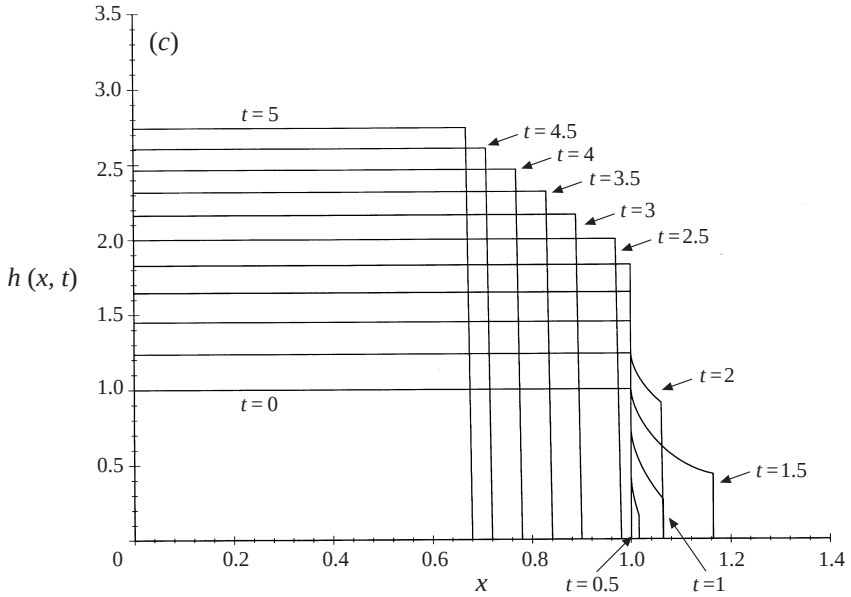

FIGURE 9. (*a*) Numerically calculated solutions for $U(t)$ for a uniform initial film in the case $E = \alpha = 1$ when the lower plate is superheated and the upper plate subcooled for $L = 1, 2, 3$; and the corresponding thin-film profiles on (*b*) the lower plate at $t = 0, 0.25, 0.5, \ldots, 1.5$ and (*c*) the upper plate at $t = 0, 0.5, 1, \ldots, 5$ in the case $L = 1$. Note that for clarity (*b*) and (*c*) use different vertical scales and are plotted at different values of t.

Typical numerically calculated solutions for $U(t)$ are shown in figure 10(*a*) for a range of values of L in the case $E = \alpha = 1$. The corresponding thin-film profiles on both plates at several different times in the case $L = 1$ are shown in figure 10(*b*) and figure 10(*c*) respectively.

Unlike the uniform initial film case considered above, condensation effects are always dominant in this case and hence the bubble always contracts. Initially, U decreases from zero until all the liquid on the superheated plate has either evaporated or been swept up by the retreating transition region. Thereafter, only condensation occurs and so the qualitative behaviour is exactly the same as in the case of a uniform initial film.

9. Conclusions

This paper investigated the mass-transfer-driven unsteady expansion and contraction of a long two-dimensional vapour bubble confined between superheated or subcooled parallel plates. It was shown that in the asymptotic limit of strong surface tension (small capillary number) the solution consists of two capillary-statics regions (in which the bubble interface is semicircular at leading order) and two thin films attached to the plates (which may dry out locally and may break up into disconnected patches of liquid), connected by appropriate transition regions. The nonlinear coupling between the profiles of the thin films and the overall expansion or contraction of the bubble was investigated for three different combinations of thermal boundary conditions and two simple initial thin-film profiles. When both plates are superheated equally, then both thin films evaporate and the bubble always expands. Depending on the details of the initial thin-film profiles, this expansion may either

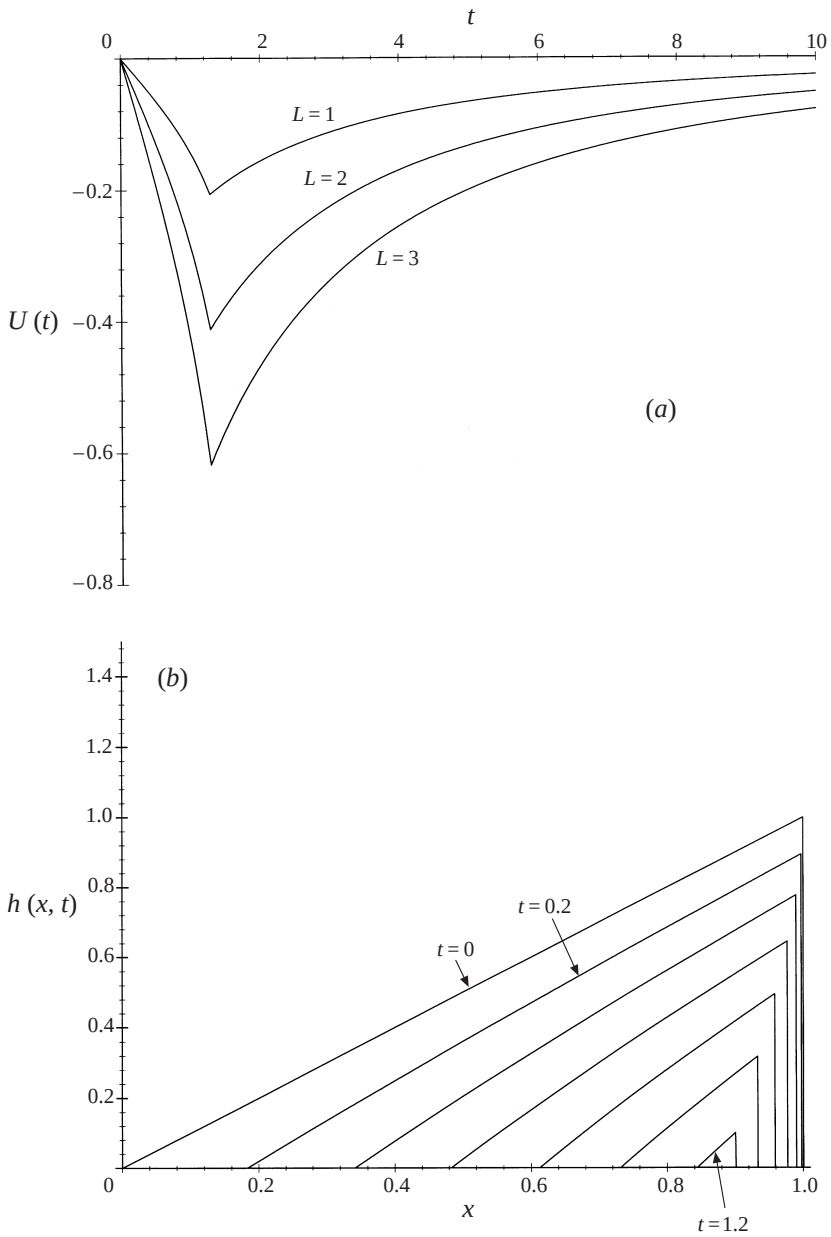

FIGURE 10(*a*, *b*). For caption see facing page.

continue indefinitely or stop in a finite time. When both plates are subcooled equally, then vapour condenses onto both thin films and the bubble always contracts. In this case the length of the thin-film region always approaches zero asymptotically in the limit $t \to \infty$. When one plate is superheated and the other subcooled with equal magnitude, then liquid evaporates from the thin film on the superheated plate and vapour condenses onto the thin film on the subcooled plate. Depending on the details of the initial thin-film profiles, either evaporation or condensation can dominate initially, and so the bubble may either expand or contract; in either case the

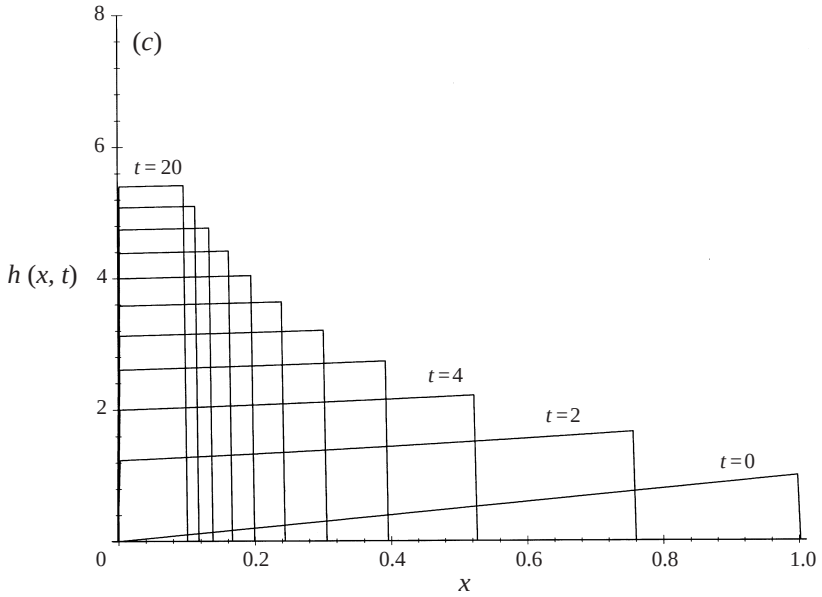

FIGURE 10. (*a*) Numerically calculated solutions for $U(t)$ for a linear initial film in the case $E = \alpha = 1$ when the lower plate is superheated and the upper plate subcooled for $L = 1, 2, 3$; and the corresponding thin-film profiles on (*b*) the lower plate at $t = 0, 0.2, 0.4, \ldots, 1.2$ and (*c*) the upper plate at $t = 0, 2, 4, \ldots, 20$ in the case $L = 1$. Note that for clarity parts (*b*) and (*c*) use different vertical scales and are plotted at different values of t.

liquid on the superheated plate will eventually either evaporate or be swept up by the retreating transition region, and so ultimately only condensation occurs and the bubble will thereafter contract and the length of the thin-film region approaches zero asymptotically in the limit $t \to \infty$, just as in the pure-condensation case.

The present work could be extended in a number of interesting ways to include, for example, situations in which the magnitude of the superheating or subcooling on the two plates is not equal, the initial thin-film profiles are not the same on both plates, the plate temperatures are non-uniform or the initial thin-film profiles are more complicated than the two simple examples considered. It might also be of interest to investigate axisymmetric versions of the present two-dimensional problem, however we do not anticipate that these problems will exhibit any qualitatively new behaviour.

As discussed in the Introduction, the main motivation for this work is to develop a simple model for the dynamics of a vapour bubble in nucleate boiling. Clearly, the next step is to construct and analyse an improved axisymmetric model in which the upper plate is removed and the bubble is allowed to expand and contract in a more realistic way.

This work was performed while the first author (S.K.W.) was a Visiting Scholar in the Department of Engineering Sciences and Applied Mathematics of Northwestern University where he was partially supported under a United States Department of Energy Grant in the Basic Energy Sciences. S.K.W. would particularly like to acknowledge the warm hospitality and stimulating academic environment provided by S.H.D. and S.G.B. during his stay at Northwestern University.

REFERENCES

Anderson, D. M. & Davis, S. H. 1995 The spreading of volatile liquid droplets on heated surfaces. *Phys. Fluids* **7**, 248–265.

Bankoff, S. G. 1994 Significant questions in thin liquid film heat transfer. *Trans. ASME: J. Heat Transfer* **116**, 10–16.

Bretherton, F. P. 1961 The motion of long bubbles in tubes. *J. Fluid Mech.* **10**, 166–188.

Burelbach, J. P., Bankoff, S. G. & Davis, S. H. 1988 Nonlinear stability of evaporating/condensing liquid films. *J. Fluid Mech.* **195**, 463–494.

Cooper, M. G. 1969 The microlayer and bubble growth in nucleate pool boiling. *Intl J. Heat Mass Transfer* **12**, 915–933.

Cooper, M. G. & Lloyd, A. J. P. 1969 The microlayer in nucleate pool boiling. *Intl J. Heat Mass Transfer* **12**, 895–913.

DasGupta, S., Schonberg, J. A., Kim, I. Y. & Wayner, P. C. 1993 Use of the augmented Young–Laplace equation to model equilibrium and evaporating extended menisci. *J. Colloid Interface Sci.* **157**, 332–342.

Dhir, V. K. 1998 Boiling heat transfer. *Ann. Rev. Fluid Mech.* **30**, 365–401.

Duffy, B. R. & Wilson, S. K. 1997 A third-order differential equation arising in thin-film flows and relevant to Tanner's law. *Appl. Math. Lett.* **10**, 63–68.

Ehrhard, P. & Davis, S. H. 1991 Non-isothermal spreading of liquid drops on horizontal plates. *J. Fluid Mech.* **229**, 365–388.

Guo, Z. & El-Genk, M. S. 1994 Liquid microlayer evaporation during nucleate boiling on the surface of a flat composite wall. *Intl J. Heat Mass Transfer* **37**, 1641–1655.

Guy, T. B. & Ledwidge, T. J. 1973 Numerical approach to non-spherical vapour bubble dynamics. *Intl J. Heat Mass Transfer* **16**, 2393–2406.

Howison, S. D., Moriarty, J. A., Ockendon, J. R., Terrill, E. L. & Wilson, S. K. 1997 A mathematical model for drying paint layers. *J. Engng Maths* **32**, 377–394.

Jawurek, H. H. 1969 Simultaneous determination of microlayer geometry and bubble growth in nucleate boiling. *Intl J. Heat Mass Transfer* **12**, 843–848.

Koffman, L. D. & Plesset, M. S. 1983 Experimental observations of the microlayer in vapor bubble growth on a heated solid. *Trans. ASME: J. Heat Transfer* **105**, 625–632.

Kotake, S. 1970 On the liquid film of nucleate boiling. *J. Heat Mass Transfer* **13**, 1595–1609.

Landau, L. & Levich, B. 1942 Dragging of a liquid by a moving plate. *Acta Physicochim. URSS* **17**, 42–54.

Lee, R. C. & Nydahl, J. E. 1989 Numerical calculation of bubble growth in nucleate boiling from inception through departure. *Trans. ASME: J. Heat Transfer* **111**, 474–479.

Mei, R., Chen, W. & Klausner, J. F. 1995*a* Vapour bubble growth in heterogeneous boiling – I. Formulation. *Intl J. Heat Mass Transfer* **38**, 909–919.

Mei, R., Chen, W. & Klausner, J. F. 1995*b* Vapour bubble growth in heterogeneous boiling – II. Growth rate and thermal fields. *Intl J. Heat Mass Transfer* **38**, 921–934.

Moosman, S. & Homsy, G. M. 1980 Evaporating menisci of wetting fluids. *J. Colloid Interface Sci.* **73**, 212–223.

Myers, T. G. 1998 Thin films with high surface tension. *SIAM Rev.* **40**, 441–462.

Oron, A., Davis, S. H. & Bankoff, S. G. 1997 Long-scale evolution of thin liquid films. *Rev. Mod. Phys.* **69**, 931–980.

Panzarella, C. H., Davis, S. H. & Bankoff, S. G. 1997 Nonlinear dynamics in horizontal film boiling. *Northwestern University Applied Mathematics Tech. Rep.* 9702. Submitted for publication.

Park, C.-W. 1992 Influence of soluble surfactants on the motion of a finite bubble in a capillary tube. *Phys. Fluids* A **4**, 2335–2347.

Park, C.-W. & Homsy, G. M. 1984 Two-phase displacement in Hele-Shaw cells : theory. *J. Fluid Mech.* **139**, 291–308.

Plesset, M. S. & Prosperetti, A. 1976 Flow of vapour in a liquid enclosure. *J. Fluid Mech.* **78**, 433–444.

Potash, M. & Wayner, P. C. 1972 Evaporation from a two-dimensional extended meniscus. *Intl J. Heat Mass Transfer* **15**, 1851–1863.

Ratulowski, J. & Chang, H.-C. 1990 Marangoni effects of trace impurities on the motion of long gas bubbles in capillaries. *J. Fluid Mech.* **210**, 303–328.

RENK, F. J. & WAYNER, P. C. 1979*a* An evaporating ethanol meniscus. Part I: Experimental studies. *Trans. ASME: J. Heat Transfer* **101**, 55–58.

RENK, F. J. & WAYNER, P. C. 1979*b* An evaporating ethanol meniscus. Part II: Analytical studies. *Trans. ASME: J. Heat Transfer* **101**, 59–62.

ROBIN, T. T. & SNYDER, N. W. 1970 Bubble dynamics in subcooled nucleate boiling based on the mass transfer mechanism. *Intl J. Heat Mass Transfer* **13**, 305–318.

SCHRAGE, R. W. 1953 *A Theoretical Study of Interphase Mass Transfer*. Columbia University Press, New York.

SCHWARTZ, L. W., PRINCEN, H. M. & KISS, A. D. 1986 On the motion of bubbles in capillary tubes. *J. Fluid Mech.* **172**, 259–275.

SNYDER, N. W. & ROBIN, T. T. 1969 Mass-transfer model in subcooled nucleate boiling. *Trans. ASME: J. Heat Transfer* **91**, 404–412.

TSUNG-CHANG, G. & BANKOFF, S. G. 1990 On the mechanism of forced-convection subcooled nucleate boiling. *Trans. ASME: J. Heat Transfer* **112**, 213–218.

TUCK, E. O. & SCHWARTZ, L. W. 1990 A numerical and asymptotic study of some third-order ordinary differential equations relevant to draining and coating flows. *SIAM Rev.* **32**, 453–469.

VAN OUWERKERK, H. J. 1971 The rapid growth of a vapour bubble at a liquid-solid interface. *Intl J. Heat Mass Transfer* **14**, 1415–1431.

VAN STRALEN, S. J. D., SOHAL, M. S., COLE, R. & SLUYTER, W. M. 1975 Bubble growth rates in pure and binary systems: combined effect of relaxation and evaporation microlayers. *Intl J. Heat Mass Transfer* **18**, 453–467.

VOUTSINOS, C. M. & JUDD, R. L. 1975 Laser interferometric investigation of the microlayer evaporation phenomenon. *Trans. ASME: J. Heat Transfer* **97**, 88–92.

WAYNER, P. C. 1993 Spreading of a liquid film with a finite contact angle by the evaporation/condensation process. *Langmuir* **9**, 294–299.

WAYNER, P. C. & SCHONBERG, J. 1992 Spreading of a liquid film on a substrate by the evaporation–adsorption process. *J. Colloid Interface Sci.* **152**, 507–520.

WILSON, S. K. 1993 The levelling of paint films. *IMA J. Appl. Maths* **50**, 149–166.

WILSON, S. K. 1995 The effect of an axial temperature gradient on the steady motion of a large droplet in a tube. *J. Engng Maths* **29**, 205–217.

ZIJL, W., RAMAKERS, F. J. M. & VAN STRALEN, S. J. D. 1979 Global numerical solutions of growth and departure of a vapour bubble at a horizontal superheated wall in a pure liquid and a binary mixture. *Intl J. Heat Mass Transfer* **22**, 401–420.